Journal of Great Lakes Research xxx (xxxx) xxx

Contents lists available at ScienceDirect

Journal of Great Lakes Research

journal homepage: www.elsevier.com/locate/ijglr

Empirical modeling of chlorophyll *a* from MODIS satellite imagery for trophic status monitoring of Lake Victoria in East Africa

Anthony Gidudu [a,*], Lydia Letaru [a], Robinah N. Kulabako [b]

[a] Department of Geomatics and Land Management, Makerere University, P.O. Box 7062, Kampala, Uganda
[b] Department of Civil and Environmental Engineering, Makerere University, P.O. Box 7062, Kampala, Uganda

ARTICLE INFO

Article history:
Received 20 December 2019
Accepted 12 May 2021
Available online xxxx
Communicated by Anthony Vodacek

Keywords:
Chlorophyll_a
Empirical modeling
Lake Victoria
MODIS

ABSTRACT

We detail our attempts at empirical modeling of MODIS derived Chlorophyll *a* (*Chl a*) distribution on Lake Victoria in East Africa and consequently its trophic status. This was motivated by the need for Lake Victoria specific algorithms, as the current satellite based standard algorithms overestimate derived *Chl a*. In situ *Chl a* data was hence collected in three field campaigns in November 2014, March 2015 and July 2015. In situ reflectances were collected during the July campaign only. We first developed models from in situ reflectances and in situ *Chl a*, which when applied to MODIS bands performed dismally (R^2 = 0.03). We then proceeded to derive empirical models by directly comparing MODIS bands with in situ *Chl a* based on data collected in November 2014 and July 2015. The March 2015 dataset couldn't be used due to cloud cover hence no matchups could be obtained. The best model derived (R^2 = 0.88) was based on the ratio 488 nm/645 nm, and was then used to determine the trophic status of Lake Victoria using Carlson's *Chl a* Trophic State Index (TSI). The results show that large areas of the lake are mesotrophic with eutrophic displays closer to the shores. The modeled TSI was then validated against in situ TSI derived from the March dataset and posted an 80% matchup. One of the main challenges, however is the prevalence of cloud cover, which hinders synoptic mapping of the lake. That notwithstanding, the study demonstrates the potential of earth observation in providing accurate TSI information for improved management of Lake Victoria.
© 2021 International Association for Great Lakes Research. Published by Elsevier B.V. All rights reserved.

Introduction

Like several other large inland lakes, Lake Victoria in East Africa is a complex system that provides a multitude of ecosystem services (Dörnhöfer and Oppelt, 2016; Gurlin et al., 2011; Olmanson et al., 2011). With a surface area of about 68,800 km^2, it is the largest fresh water lake in Africa and is shared by Uganda (43%), Kenya (6%) and Tanzania (51%) (Chapman et al., 2008). Not only does Lake Victoria support a rich diversity of flora and fauna (Cavalli et al., 2009), but it also provides a variety of ecosystem services such as being a source of potable water and water for irrigation, fisheries, recreation, transportation etc. (Balirwa, 2007; Carvalho et al., 2013). Similar to other inland lakes, Lake Victoria's water quality has over the years been continually compromised by cultural eutrophication (Gurlin et al., 2011) as a result of inappropriate agricultural practices, indiscriminate disposal of wastes, increasing population pressure, industrialization etc. (Chavula et al., 2009, Dörnhöfer and Oppelt, 2016, Duan et al., 2012).

One of the standard water quality parameters of interest to the various stakeholders involved in the management of inland lake resources and coastal waters is Chlorophyll_a (*Chl a*) (Lacava et al., 2018; Moses et al., 2009; Watanabe et al., 2018). *Chl a* is a photosynthetic pigment found in phytoplankton and therefore measuring *Chl a* gives a measure of phytoplankton biomass and hence the productivity of the lake (Garaba et al., 2014; Laliberté et al., 2018; Moses et al., 2009).

The conventional approach to measuring *Chl a* in lakes and other water bodies of interest involves standardized in situ approaches where at a given location of interest a water sample is collected and filtered under low vacuum through Whatman filters (Garaba et al., 2014). The filter is then stored, until it can be further analyzed in the laboratory to determine the *Chl a* concentration for that location (Nasr et al., 2007). This approach gives accurate results; and, if sufficiently consistent, can be used for scientific research and long term monitoring (Erkkilä and Kalliola, 2007). Unfortunately, this conventional approach to monitoring *Chl a* is labor intensive, cumbersome, cost prohibitive, with limited sample collection over temporal and spatial scales (Bierman et al., 2011; Reyjol et al., 2014; Schaeffer et al., 2013). Given the dynamic

* Corresponding author.
E-mail address: anthony.gidudu@mak.ac.ug (A. Gidudu).

https://doi.org/10.1016/j.jglr.2021.05.005
0380-1330/© 2021 International Association for Great Lakes Research. Published by Elsevier B.V. All rights reserved.

Please cite this article as: A. Gidudu, L. Letaru and R.N. Kulabako, Empirical modeling of chlorophyll *a* from MODIS satellite imagery for trophic status monitoring of Lake Victoria in East Africa, Journal of Great Lakes Research, https://doi.org/10.1016/j.jglr.2021.05.005

nature of inland lakes, and more importantly, the essential nature of the ecosystem services lakes provide for human welfare, there is an urgent need to monitor the lakes at finer spatial–temporal scales (Gurlin et al., 2011; Hestir et al., 2015; Schaeffer et al., 2013).

The most prominent new strategy to assist in the sustainable management of inland waters has been the adoption of satellite imagery to monitor water quality (Chavula et al., 2009, Gurlin et al., 2011). Satellite images through remote sensing of the water bodies from space mitigate against the shortcomings of conventional monitoring methods by providing near-real time synoptic coverage and temporal consistency of data (Schaeffer et al., 2013; Zheng and Giacomo, 2017). It also has the potential to provide crucial long-term archival data on inland and near-coastal transitional waters in locations where conventional water-quality monitoring programmes are either absent or unsatisfactory (Navalgund et al., 2007). Some of the satellite sensors that have been deployed for monitoring of water quality include the Coastal Zone Color Scanner (CZCS) (Gordon et al., 1983), Sea-viewing Wide Field-of-View Sensor (SeaWiFS) (Hooker and McClain, 2000), the Moderate Resolution Imaging Spectroradiometer (MODIS) (Esaias et al., 1998), MEdium-spectral Resolution Imaging Spectrometer (MERIS) (Dekker et al., 1991) and more recently, Sentinal-3 (Gómez-Jakobsen et al., 2016), among others.

The derivation of water quality parameters from satellite imagery is based on algorithms such as the standard National Aeronautics and Space Administration's (NASA) empirical algorithms (O'Reilly et al., 1998, 2000; Werdell and Bailey, 2005; Hu et al., 2012). These algorithms are developed through bio-optical modeling which refers to the determination of the optical property of a water body as a function of the biological activity within the water body (Morel, 2001). The ability to detect *Chl a* concentration through remote sensing is vested in the fact that it is a photoactive pigment which causes distinct changes in the color of water by absorbing and scattering light incident on the water (Moses et al., 2009). The concentration of *Chl a* can thus be estimated from remote sensing reflectance by relating optical changes observed in the reflected light at specific wavelengths to the in situ measurement of *Chl a* (Matthews, 2011; Moses et al., 2009). Remote sensing reflectance in this case refers to the ratio of the radiance backscattered to the direct solar radiation incident on the water surface, which represents the 'spectral signature' of the water and integrates the spectral absorption and backscattering properties of all the materials present in the water column (Coble et al., 2004). Typically, the constituents responsible for color of any water body include Colored Dissolved Organic Matter (CDOM), Suspended Particulate Matter (SPM) and *Chl a* (Garaba et al., 2014). In cases where phytoplankton is the predominant constituent and the concentrations of other constituents co-vary with *Chl a* concentration, those water bodies are referred to as Case I waters (Gordon and Morel, 1983). Thus, the optical properties of these waters are dominated by phytoplankton and the observed spectral features in the light detected by the satellite sensor can be directly solely related to *Chl a* concentration (Moses et al., 2009). Examples of case I waters include the open ocean, coastal areas without a continental shelf and input of terrigenous particles and in some upwelling regions (Gordon and Morel, 1983). Inland lakes and coastal areas with a continental shelf on the other hand fall under the category of case II waters where constituents such as suspended solids and dissolved organic matter occur in abundance and their concentrations do not co-vary with *Chl a* concentration (Moses et al., 2009). Thus phytoplankton does not solely dominate the optical properties of such turbid productive waters and are described as being optically complex waters (Morel and Prieur, 1977).

The current existing standard algorithms for the derivation of *Chl a* have principally been designed for Case I waters; and studies have shown that when applied to Case II waters, they have not yielded accurate results (Gómez-Jakobsen et al., 2016; Lacava et al., 2018; Lesht et al., 2012). For example when applied to case II waters like inland lakes, *Chl a* is mostly over estimated (Lessin et al., 2009; Matthews et al., 2012; Mustapha et al., 2012). In a study on Lake Victoria by Gidudu et al. (2018), match ups were made between in situ *Chl a* measurements and MODIS derived retrievals of *Chl a*. The findings indicated that satellite derived *Chl a* was over estimated when compared to the corresponding in situ observations. From these studies, there has been a strong case about the need to develop algorithms best suited for specific case II waters (Gurlin et al., 2011; Lesht et al., 2012). Examples of Case II specific algorithms developed in response to this include the Yellow River in China (Chen and Quan, 2013), the Alboran Sea located between the Iberian Peninsula and the north of Africa (Gómez-Jakobsen et al., 2016), St. Lawrence Estuary and Gulf in Canada (Laliberté et al., 2018) and the Great lakes of North America (Lesht et al., 2013).

Empirical modeling involves the comparison of in situ *Chl a* concentration with single bands, band ratios, band arithmetic or multiple bands as independent variables in linear, multiple linear or non-linear regression analyses (Dahanayaka et al., 2014; Duan et al., 2008; Matthews, 2011; Rundquist et al., 1996). The resultant regression equation is then applied to every pixel in the satellite image depicting the spatial distribution of *Chl a* retrieval from the satellite image scene (Matthews, 2011). The remotely sensed signal used in empirical modeling may be obtained from a portable spectrometer or a satellite image. Portable spectrometers may be handheld or attached to a vessel and are deployed to carry out reflectance measurements above the water surface (Jiao et al., 2006; Thiemann and Kaufmann, 2000; Rundquist et al., 1996). Portable spectrometers are hyperspectral (i.e. are able to measure reflectances across several bands of spectra) with the advantage of being able to record extremely narrow wavebands allowing for detection of very small variations in received energy (Dahanayaka et al., 2014). In situ reflectances are usually used to calibrate, validate and improve the modeling of *Chl a* from satellite imagery. The principle of satellite based *Chl a* modeling involves relating the satellite bands with measured in situ *Chl a* concentration (Dahanayaka et al., 2014; Ritchie et al., 2003). To account for the altitude of the satellite sensor above the water body, requisite atmospheric corrections are applied. Empirical modeling has the advantage of computational simplicity and ease of implementation (Dörnhöfer and Oppelt, 2016; Lesht et al., 2012; Matthews, 2011), however its application is restricted to a specific location or sensor (Giardino et al., 2010). That said, the increasing number of recent studies using empirical modeling proves that empirical algorithms have the capacity to provide reliable information on inland and transitional waters (Matthews, 2011).

One of the principal purposes of determining *Chl a* distribution in water bodies is to be able to establish the trophic status of the lake. Trophic status is defined as the total weight of biomass in a water body at a specific location and time (Baban, 1999; Murthy et al., 2008; Prasad and Siddaraju, 2012). It refers to the biological response for nutrient additions to the water bodies (Naumann,1929) and is useful in measuring water quality because it relates directly to both human-use perceptions of quality and to the abundance of algae (Ziboon et al., 2010). Various methods have been adopted for the classification of lakes and to indicate their trophic status (Galvez-Cloutier and Sanchez, 2007; Murthy et al., 2008) such as OECD (1982), Nürnberg (1996) criteria; National Sanitation Foundation Water Quality Index for the assessment of water quality in the United States; Water Quality Index of Canada (Rocchini and Swain, 1995) and Carlson's Trophic State Index (TSI) (Carlson, 1977). Of these different approaches, the most common method for characterizing a lake's trophic status or overall health is the Carlson's Trophic State Index (TSI) (Murthy et al., 2008; Prasad and Siddaraju, 2012). TSI is widely accepted owing to its

Table 1
Carlson's TSI classification and nomenclature (Carlson, 1977).

TSI	Classification	Description
<30–40	Oligotrophic	• Clear water, dissolved oxygen throughout the year in hypolimnion • Deep lakes still exhibit classical oligotrophy, but some shallower lakes will become anoxic in the hypolimnion during summer
40–50	Mesotrophic	• Water moderately clear, but increasing probability of anoxia in hypolimnion during summer
50–70	Eutrophic	• Lower boundary of classical eutrophic; decreased transparency, anoxic hypolimnion during summer, macrophyte problems evident, and warm-water fisheries only • Dominance of blue-green algae, algae, algal scum probable, extensive macrophyte beds, but extent limited by light penetration
70–80>	Hyper-eutrophicHyper-eutrophic	• Heavy algal blooms possible throughout the summer, dense macrophyte beds, but extent limited by light penetration • Algal scum, summer fish kills, few macrophytes, dominance of rough fish

computational simplicity and ability to communicate between researchers, government agencies, and local community residents (Carlson, 1977). Carlson's TSI depends on algal biomass as the basis for the trophic status classification, and can be independently estimated from any (or all) of the following parameters: *Chl a*, Secchi Depth (SD) and Total Phosphorus (TP) (Baban, 1999; Prasad and Siddaraju, 2012; Zhengjun et al., 2008); however, in this paper we focus on *Chl a*. *Chl a* measurement indicates how much algae are present in the water, and so gives an indication about the quantity of nutrient present in the sampled water (Murthy et al., 2008). TSI is categorized into a continuum dividing trophic state into three conventional main classes namely: oligotrophic (i.e. low nutrient enrichment), mesotrophic (moderate nutrient enrichment) and eutrophic (high nutrient enrichment) (Brown and Simpson, 2001; Murthy et al., 2008). Carlson's TSI for lakes yields continuous values scaled between 0 and 100, with the advantage that it is numeric in nature allowing for more categories to be grouped into the conventional nomenclature classes illustrated in Table 1 (Carlson, 1977).

The adoption of satellite imagery in TSI determination is premised on the fact that the consequences of eutrophication and an increase in productivity affect the chromatic optical properties and water quality of lakes (Baban, 1999; Tian and Ni, 1988). For instance, increases of *Chl a* are related to a significant decrease in the relative amount of energy in the blue wavelength (0.45–0.52 nm) and an increase in the green wavelength (0.52–0.60 nm) (Clarke et al., 1970). Similarly, an increase in suspended solids in the water will result in a decrease in Secchi depth which will lead to an increase in the reflected energy, and consequently the peak of reflectance will move towards the longer wavelengths (Lillesand and Kiefer, 1994). These changes are discernable through measurement using portable spectrometers and satellite imagery, hence providing the means for modeling eutrohication degree of (Baban, 1999; Clarke et al., 1970). The purpose of this current paper therefore, is to explore means by which *Chl a* can be empirically modeled using in situ and MODIS satellite based reflectance measurements to improve trophic status assessment on Lake Victoria in East Africa.

Methods

In situ data collection

This paper is based on the results of three field campaigns that were carried out on the Ugandan portion of Lake Victoria as shown in Fig. 1. In the first two field campaigns dated 26 November 2014 and 12 – 13 March 2015 only in situ *Chl a* was collected and for the third field campaign dated 27 – 28 July 2015 both in situ *Chl a* and in situ reflectances were collected at each sampling point. Sampling points were approximately 2 km apart. The data was collected such that at each sampling point, location was determined using a handheld GPS to enable co-location with corresponding positions on the satellite imagery. In keeping with similar studies (e.g. Kahru et al., 2014; Lacava et al., 2018; Mustapha et al., 2012), in situ sampling was carried out three hours before and after satellite overpass (i.e. between 11:30 am and 5:30 pm). Sampling was also done to ensure that the sampling points were at least 1 km from the shoreline to avoid possible influence from direct runoff and river plumes, as well as to avoid the effects of land adjacency (Kahru et al., 2014).

At each sampling point, water samples were collected from the surface of the lake using a Van Dorn sampler. The samples were then filtered aboard the vessel using a glass microfiber GF/C Whatmann filter with a diameter of 47 mm and nominal pore size of 1.2 μm. The filters were then immediately transferred to aluminum foil folders containing activated silica gel to keep them dry and then kept away from direct sunlight to prevent pigment degradation (Stainton et al., 1977). The gel was changed every day until the filters were delivered to the laboratory whereupon they were frozen immediately. Extraction of frozen filter was done within 48 h on return using the hot ethanol spectrophotometric method (ISO10260: 1992).

In situ reflectances at each sampling location were collected using a portable handheld Ocean Optics Jaz Spectrometer fitted with a cosine corrector, with a spectral resolution of 0.3 nm and a spectral range from 339 nm to 1022 nm. The protocol used was that at each station the spectrometer was pointed vertically up to the source of light (sun), then a dark measurement was taken to carry out internal calibration then the spectrometer was pointed perpendicular to the water surface to take the sample measurement. Caution was taken to capture spectra away from sun glint and boat shadow (Thiemann and Kaufmann, 2000). The reflected radiation field over the collected samples in the different stations was assumed to be Lambertian (Lacava et al.,2018). We used the spectral range of 400 nm to 750 nm in keeping with best practices to reduce on the impact of spectral noise contamination (Rundquist et al., 1996; Schalles et al., 1998).

Satellite imagery

MODIS Aqua imagery was used in this work to retrieve satellite based reflectances, and was accessed through the National Aeronautics and Space Administration (NASA) Ocean Colour Website (oceancolor.gsfc.nasa.gov). We used Level 2 reflectance images coinciding with the days of the in situ field campaigns. Level 2 imagery is processed from raw spectroradiometer data and has been atmospherically corrected using the standard Near Infra-Red (NIR) atmospheric correction algorithm (Gordon and Wang, 1994; McClain, 2009), which employs the NIR black pixel assumption in open oceans (Wang et al., 2012). Corresponding match ups were available for in situ data collected on the 26 November 2014 and 27 July 2015. There was no available imagery over the sampled

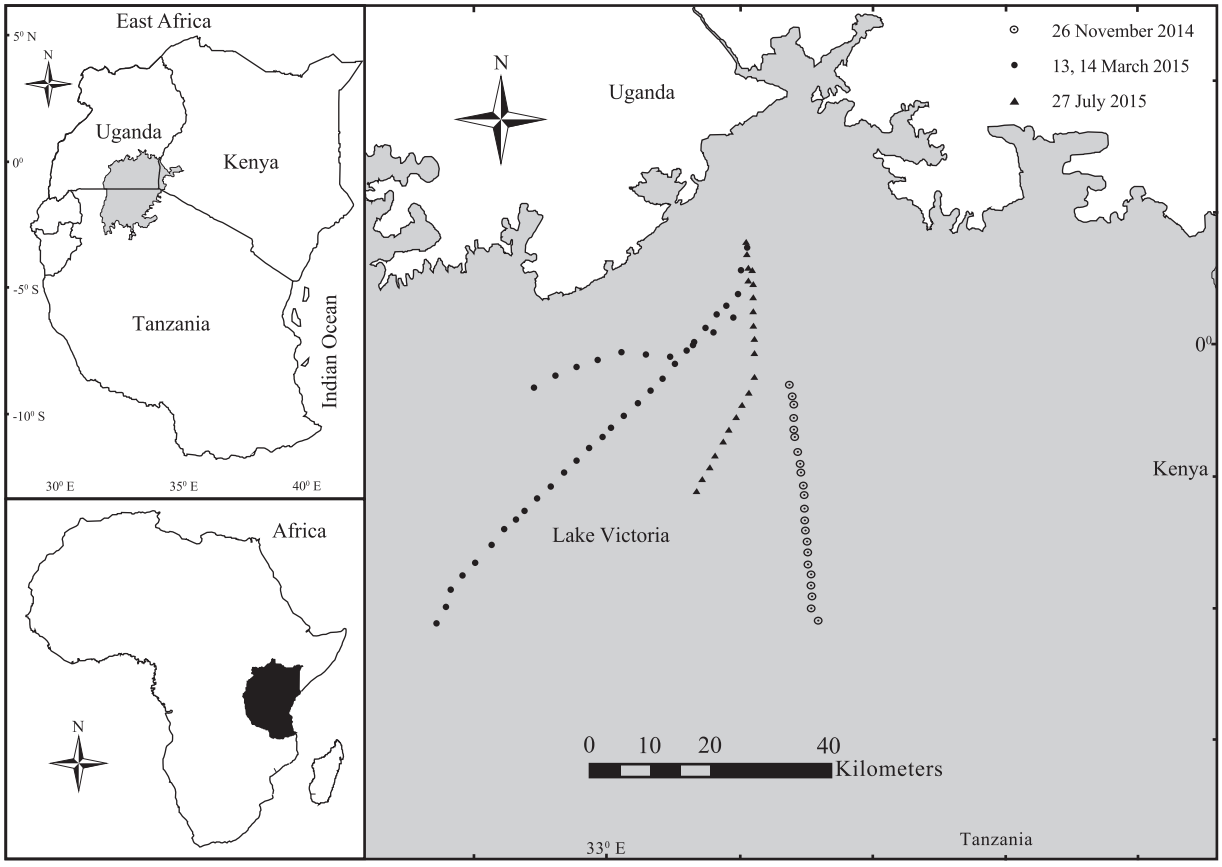

Fig. 1. Study area with expedition routes.

areas on the 12 – 13 March 2015 due to cloud cover, however the dataset was later used to validate derived TSI.

Modeling of Chl a

Fig. 2 gives a schematic representation of how lake specific modeling of *Chl a* was performed. The first step was to identify the best wavelengths to use in model development. Two methods were used in this regard. In the first method, correlation was made between in situ *Chl a* measurements and in situ reflectances taken using the Jaz spectrometer at each point (Dahanayaka et al., 2014). The wavelengths with the strongest positive and negative correlations were then selected for modeling the relationship (Jiao et al., 2006). The choice of correlation test to use between Pearson, Kendall, and Spearman's rank correlation tests was determined by the Kolmogorov–Smirnov one-sample test (Garaba and Zielinski, 2015). The second approach involved getting the standard deviations of reflectances at each wavelength and comparing them to in situ *Chl a* concentration. The wavelengths at which the largest and lowest standard deviations occurred were taken as the best regions for modeling the relationship between in situ reflectances and in situ *Chl a* (Schalles et al., 1998). The wavelengths from the two methods were then used to create regression models with respect to in situ *Chl a*.

For each of the regression models developed, they were assessed according to coefficient of determination (R^2) which is used as a measure of covariance that captures the proportion of variance in one variable that can be predicted from another (Kahru et al., 2014). Other error matrices considered included the Root Mean Square Error (RMSE) (See Eq. (1)); uncertainty parameters, such as bias, i.e. Mean Absolute Deviation (MAD) (see Eq. (2)) and measures of scatter, in this case, Mean Absolute Percent Error (MAPE) (See Eq. (3)). The choice of these error matrices was premised on existing literature on similar studies, such as Brewin et al. (2015), Garaba and Zielinski (2015) and Kahru et al. (2014).

$$\mathrm{RMSE} = \sqrt{\frac{\sum_{i=1}^{n} |X_i - X_s|^2}{n}} \tag{1}$$

$$\mathrm{MAD} = \frac{\sum_{i=1}^{n} |X_i - X_s|}{n} \tag{2}$$

$$\mathrm{MAPE} = \sum_{i=1}^{n} \frac{|X_i - X_s|}{X_i} \tag{3}$$

where X_i are the in situ observations, X_s the corresponding modeled *Chl a* and n the number of valid match-ups.

The model yielding the best statistics was then applied to the corresponding MODIS bands. The modeled satellite derived *Chl a* was compared with the in situ *Chl a* based on coefficient of determination and Eqs. (1)–(3). In the case that the results were unsatisfactory, regression models were developed using the MODIS bands directly.

Trophic status modeling

The regression algorithm with the best statistics was then used to model *Chl a* from MODIS imagery and then converted to TSI(Chl) values according to Eq. (4). Daily *Chl a* images were binned and

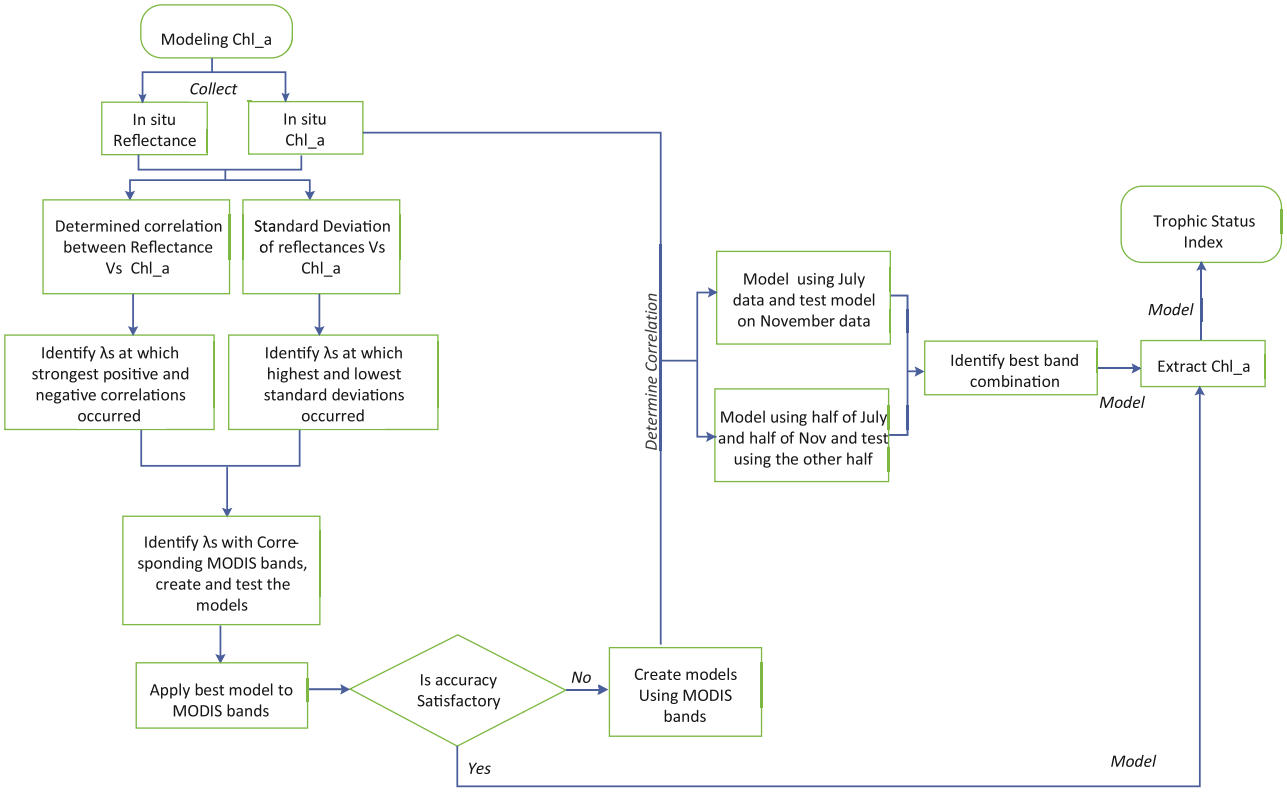

Fig. 2. Schematic representation of Chl *a* modeling.

converted to monthly *Chl a* composite images which were then converted into monthly trophic status maps.

$$TSI(Chl) = 10(6 - \frac{2.04 - 0.68\ln(Chla)}{\ln(2)}) \quad (4)$$

(Carlson, 1977)

Results and discussion

Modeling Chl a using in situ reflectances

During the field campaign carried out on 27 July 2015, 22 in situ *Chl a* and corresponding reflectance measurements were sampled. The Kolmogorov–Smirnov one-sample test showed that the in situ *Chl a* concentrations were normally distributed hence correlations were evaluated based on Pearson's Product Moment correlation test. The first attempt at identifying the best wavelengths for modeling *Chl a* involved plotting the correlation between in situ reflectances with in situ *Chl a* concentrations against wavelength as shown in Fig. 3.

The importance of Fig. 3 was to enable the identification of areas of strong correlation and using those wavelengths to model *Chl a* concentrations. The highest positive correlation was identified between 545 and 587 nm with the highest at 581 nm and highest negative correlation occurred between 408 and 436 nm with the peak at 409 nm. These results are similar to those of Fuli et al. (2004), whose strongest positive correlation was between 545 nm and 587 nm, though their strongest negative correlation was in the range of 440 nm – 499 nm. The results are also similar to Rundquist et al. (1996) who identified the best wavelengths for modeling *Chl a* to be between 530 nm and 600 nm. Similar studies have identified respective positive and negative correlations as follows: 667 nm and 719 nm (Jiao et al., 2006), 680 nm and 708 nm (Thiemann and Kaufmann, 2000), 679 nm and 706 nm (Li et al., 2002). The difference between our results and these studies could be attributed to the fact that their studies considered highly eutrophic water bodies with significantly higher concentrations of *Chl a* than Lake Victoria.

The second approach of identifying the candidate wavelengths to be used in modeling *Chl a* concentration involved analyzing the plotting of standard deviation of reflectance at each wavelength against wavelength. The wavelength's of interest are the wavelengths at which standard deviations are highest and lowest (Schalles et al., 1998). From Fig. 3, the wavelength at which the highest standard deviation occurred between 400 and 430 nm with the maximum of 0.35 at 404 nm and the least standard deviation occurred between 500 and 600 nm with the minimum of 0.04 at 547 nm. Whereas Schalles et al. (1998) obtained a standard deviation of 0.4 nm between 400 nm and 450 nm, similar to ours, their highest and lowest standard deviation occurred 700 nm and 670 nm, as opposed to ours which occurred at 404 nm and 547 nm respectively. We again postulate that these differences were due to the different ranges of *Chl a* under consideration with Schalles et al. (1998), ranging between 20 mg/m^3 to 280 mg/m^3.

The aim of this process was to identify the best wavelengths from in situ reflectance measurements for modeling *Chl a*, and developing models to be applied on MODIS satellite imagery. We therefore had to select in situ reflectances which corresponded with the MODIS bands. Of the identified reflectances, 581 nm had no equivalent MODIS band, the wavelength at 409 nm corresponded with band 8 and 547 nm corresponded with band 12. The wavelength 404 nm was also considered since it was within 2 nm of the MODIS bands (O'Reilly et al., 1998) (band 8 in this case).

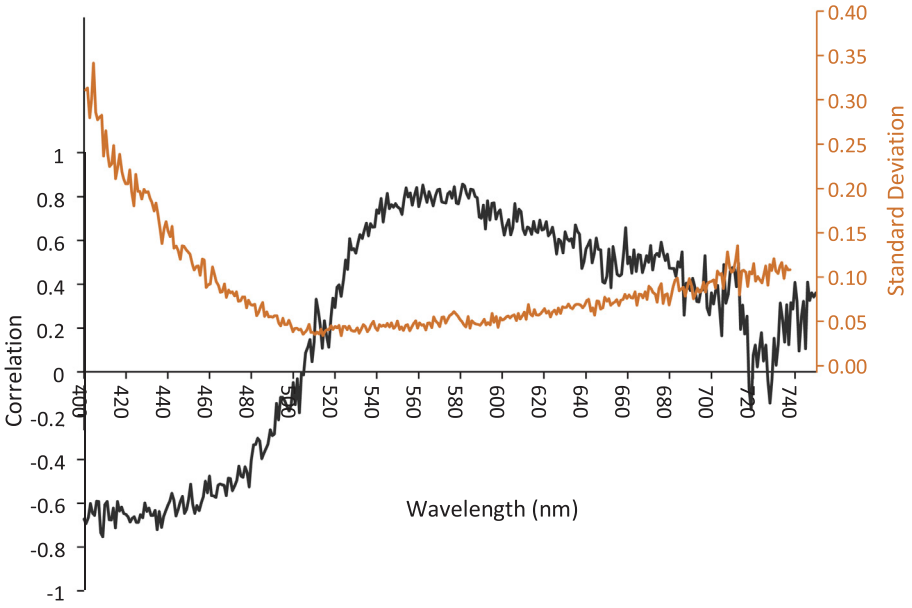

Fig. 3. Variation of the Correlation and Standard Deviation with wavelength.

Table 2
Empirical modeling using test data of 27th July 2015 and validation against data collected on the 20th November 2014.

Model	Equation	Ratio	Model R^2	Validation R^2	n	MAD	MSE	RMSE	MAPE
Y1	log(y) = −2.60 log(x) + 1.14	488/645	0.90	0.57	12	1.86	3.55	1.89	0.39
Y2	log(y) = −3.13 log(x) + 1.34	488/678	0.87	0.21	12	2.69	7.44	2.73	0.56
Y3	log(y) = −3.07 log(x) + 1.32	488/667	0.85	0.03	12	2.37	5.79	2.40	0.49
Y4	log(y) = −2.67 log(x) + 1.02	531/645	0.83	0.11	12	2.26	5.24	2.29	0.47
Y5	log(y) = −7.51 log(x) + 1.08	469/645	0.82	0.35	12	2.66	7.29	2.70	0.56

Empirical modeling then proceeded using the ratios and natural logs of the ratios as follows: R_{rs}(409 nm/547 nm), R_{rs}(404-nm/547 nm), log R_{rs}(409 nm/547 nm), log R_{rs}(404 nm/547 nm). The ratio of R_{rs}(404 nm/409 nm) was not considered because in MODIS they correspond to the same band 8. The results showed that when compared to in situ *Chl a* there was an improvement in the R^2 statistic for 404 nm/547 nm and 409 nm/547 nm when logarithmic ratios were used. The R^2 for 404 nm/547 nm improved from R^2 = 0.49 to R^2 = 0.58 while the R^2 for 409 nm/547 nm improved from R^2 = 0.65 to R^2 = 0.72. This improvement when using logarithmic scales is is similar to results of Harma et al. (2001). From the results of the in situ empirical modeling of *Chl a*, we identified the best ratio as log(409 nm/547 nm) with the regression Eq. (5):

$$y = -1.47x + 1.14 \tag{5}$$

where y = log (In situ *Chl a*) concentration being modelled, and × = log of the ratio of Standardized reflectances at 409 nm and 547 nm.

Modeling Chl a concentration from MODIS imagery

To test the regression model on satellite imagery, same day match ups were made between the in situ locations and MODIS satellite bands 8 (R_{rs} 409) and 12 (R_{rs} 547) of the data collected on 27 July 2015. Of the original 22 sampling locations, only 15 could be used for testing the model, the rest having been rendered unsuitable by falling within the cloud-ice mask and straylight mask. When Eq. (5) was applied to the satellite derived reflectances and the derived *Chl a* concentration compared with in situ concentration at the test locations, it yielded the following statistics:

$$MAD = 381.60; MSE = 175505.20; RMSE = 418.93; MAPE = 48.61; R^2 = 0.03 \tag{6}$$

From the results in Eq. (6), it is evident that the derived model has performed very poorly, which could be attributed to influence of the atmosphere (Matthews et al., 2010), hence the possible need for requisite atmospheric algorithms to match the model.

Having failed to identify an in situ model that could be applied on the satellite, we set out to carry out empirical modeling of *Chl a* concentration relating in situ *Chl a* with MODIS bands 8 to 14. This approach has precedence in literature e.g. Duan et al. (2008), where having failed to get appropriate satellite bands basing on in situ reflectance modeling, proceeded to do *Chl a* modeling using the satellite bands directly. The first empirical modeling attempt involved modeling using data collected on the 27 July 2015, and validating it against data collected during the field campaign on the 20 of November 2014, the results of which are depicted in Table 2. Table 2 gives the best 5 log ratios obtained.

As can be seen from Table 2, the results were at best moderate with model Y1 yielding the best results. The results for Models: Y2, Y3, Y4 and Y5 yielded significantly poorer results. The poor results could be due to the difference in the atmospheric and physical conditions (e.g. changes in the phytoplankton population in different seasons) during the modeling and validation periods (Matthews et al., 2010; Ritchie et al., 2003; Mueller, 2000). In our case, the modeling dataset collected in July 2015 was in the middle of the dry season, while the validation dataset of November 2014 was collected towards the end of a rainy season.

The next attempt involved developing models using half of the data of both sampling dates and validating the results on the other

half i.e. developing empirical models using half of the available data on the 27 July 2015 and half of the data of 20 November 2014 and validating it on the other half. The aim of this was to capture the range of in situ data variability on both days in the model. Table 3 summarizes the best 4 statistical results of the modeling. From Table 3, model Y6 performed best with very strong coefficients of determination and minimal errors. The strong R^2 meant that model Y6 was best suited for modeling the relationship between in situ *Chl a* and MODIS derived Rrs over the two months and was consequently used to model *Chl a* variation on Lake Victoria and finally carry out trophic status mapping.

As observed in Tables 2 and 3, the ratio 488 nm/645 nm posted the best results, indicating that we found stronger correlations between *Chl a* and blue/red reflectance ratios, which is different from the standard Ocean Colour algorithms that are based on the blue/green ratios. It is posited that the principle behind the blue/red ratio is that both bands correspond to *Chl a* absorption and as the concentration of *Chl a* in the water body increases, the reflectance in both blue and red spectrum decreases (Han and Jordan, 2005). However, the rate of decrease in red was faster than the one in blue. Han and Jordan (2005) further argue that since the reflectance of the red band is also affected by inorganic suspended sediments and dissolved organic matter, the ratio of blue and red may work effectively in estimating *Chl a* only when the *Chl a* concentration is higher than a certain level and the turbidity of water is relatively low. Similarly, Gitelson et al. (1996) found the ratio of red/blue, a reciprocal ratio of blue/red, was effective in estimating *Chl a* concentrations greater than 3 mg/m^3.

Trophic status mapping

The first step to mapping the trophic status of Lake Victoria, involved determining the spatial distribution of *Chl a* variation using the empirical model Y6. To get monthly composite images, *Chl a* variation for each day was modelled and then binned to form a monthly composite. The monthly *Chl a* images were then converted to the TSI(Chl) using equation (4) and consequently classified according to TSI Classifications in Table 1. The mapping was applied only for the months of November 2014 (Fig. 4a) and July 2015 (Fig. 4c) and the consequent TSI Classifications respectively depicted in Fig. 4b and d.

One of the main challenges in the use of satellite imagery for mapping is cloud cover which obscures mapping areas of interest, which is why the maps have unmapped patches. However from the areas that could be mapped, the lake is largely mesotrophic in the middle, with eutrophic characteristics closer to the shores. We also determined the TSI for the month of March 2015 and compared the results with in situ results collected on the 12 – 13 March 2015. This dataset could not be used for model development due to cloud cover on those two days. A *Chl a* monthly composite for the month of March was classified using this derived model and the results compared with in situ TSI for the two dates. The results are shown in Table 4, and they demonstrate an 80% match between the modeled and in situ TSI. Where the classification differs, it is with a difference of one class, with the model over estimating TSI. This difference may be attributed to the fact that the satellite derived

Table 3
Empirical modeling using test data of (27th July 2015 and 20th November 2014) and validation data of 27th July 2015 and 20th November 2014).

Model	Equation	Ratio	Model R^2	Validation R^2	n	MAD	MSE	RMSE	MAPE
Y6	log(y) = −1.52 log(x) + 1.05	488/645	0.90	0.88	13	0.82	1.07	1.03	0.12
Y7	log(y) = −1.4 log(x) + 1.11	488/678	0.86	0.79	13	0.97	1.61	1.27	0.14
Y8	log(y) = −1.51 log(x) + 1.12	488/667	0.86	0.83	13	0.92	1.40	1.18	0.13
Y9	log(y) = −1.37 log(x) + 0.97	469/645	0.88	0.81	13	1.01	1.56	1.25	0.14

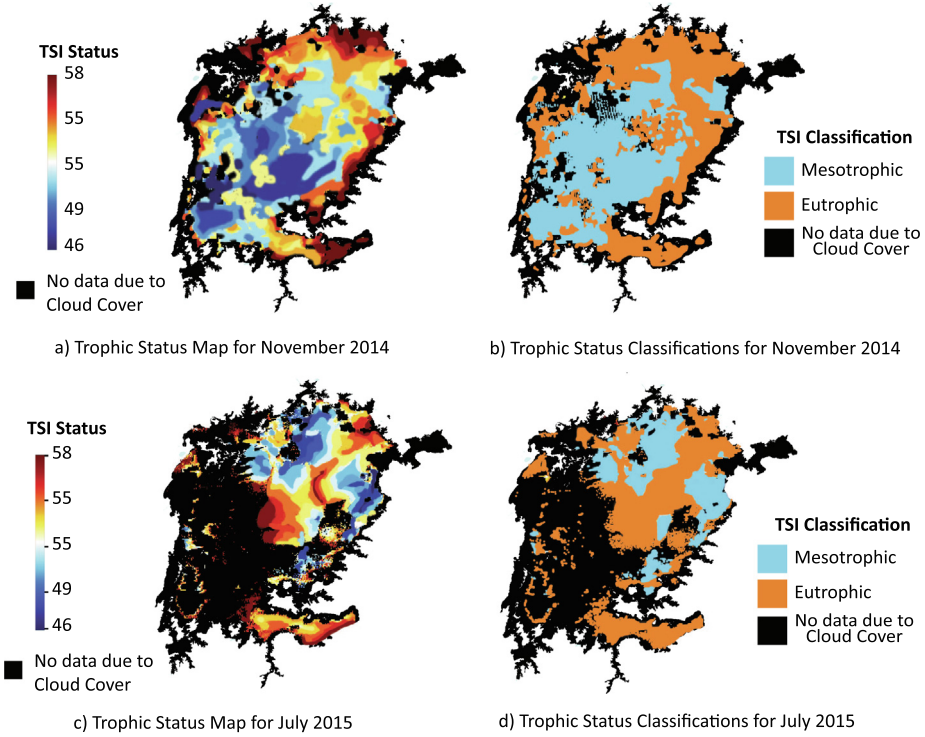

Fig. 4. Modeling of Monthly averaged Trophic Status Index (TSI) and TSI Classifications.

Table 4
Comparison of in situ determined and modeled with Trophic Status indicated.

Latitude	Longitude	Chl_a$_{In\ situ}$	TSI(Chl)$_{In\ situ}$	Chl_a$_{modeled}$	TSI(Chl)$_{modeled}$
0.031	33.195	7.5	Eutrophic	8.0	Eutrophic
−0.001	33.132	6.2	Mesotrophic	7.2	Eutrophic
−0.022	33.091	4.2	Mesotrophic	4.5	Mesotrophic
−0.011	33.059	2.6	Mesotrophic	5.2	Mesotrophic
−0.011	33.028	2.9	Mesotrophic	8.2	Eutrophic
−0.032	33.101	6.2	Mesotrophic	4.5	Mesotrophic
−0.011	33.122	5.9	Mesotrophic	5.2	Mesotrophic
−0.001	33.132	9.5	Eutrophic	7.2	Eutrophic
0.020	33.153	6.5	Eutrophic	8.8	Eutrophic
0.041	33.164	8.5	Eutrophic	8.7	Eutrophic

TSI(Chl) is modeled from monthly data and is being compared to in situ TSI(Chl) collected on one day.

Conclusions

This research presents the first attempt at determining the Trophic Status Index of Lake Victoria through empirical modeling of *Chl a* from MODIS satellite imagery. We first set out to establish the best model using in situ *Chl a* and in situ reflectances observations however when applied to MODIS bands, the results were unsatisfactory, and we postulate that this could be due to not accurately modeling atmospheric corrections. We then decided to model *Chl a* using the MODIS bands directly. The resulting model that we derived was based on the ratio 488 nm/645 nm i.e. blue to red ratio similar to Han and Jordan (2005). When this model was used to extract TSI, it yielded comparable results to in situ TSI observations. The import of this is that, we can accurately model TSI from MODIS imagery which can be accessed regularly, cost effectively, offering synoptic coverage of the lake as opposed to using in situ measurements which are costly to collect regularly and are limited in space and time. These results present a foundation upon which improved modeling can be advanced, as more data is collected. We envisage that this research will make a contribution towards the operationalization of the use of satellite imagery in monitoring water quality on Lake Victoria, by providing regular, accurate and reliable data for the management of the lake.

Declaration of Competing Interest

The authors declare that they have no known competing financial interests or personal relationships that could have appeared to influence the work reported in this paper.

Acknowledgements

The authors acknowledge the financial support of the Norwegian Agency for Development Cooperation (NORAD) - Norwegian Programme for Capacity Development in Higher Education and Research for Development (NORHED I) under the WaSo Africa Project – Institutional Capacity Building in Water Resource Management and Climate Change Adaption under Grant Number QZA-0485-13/0021. We also acknowledge the feedback from the reviewers, whose comments greatly improved the original manuscript.

References

Baban, J.M.S., 1999. Use of remote sensing and geographical information systems in developing lake management strategies. Hydrobiologia 395 (396), 211–226.
Balirwa, J.S., 2007. Ecological, environmental and socioeconomic aspects of the Lake Victoria's introduced Nile perch fishery in relation to the native fisheries and the species culture potential: lessons to learn. Afr. J. Ecol. 45, 120–129.
Bierman, P., Lewis, M., Ostendorf, B., Tanner, J., 2011. A review of methods for analysing spatial and temporal patterns in coastal water quality. Ecol. Indic. 11, 103–114.
Brewin, R.J.W. et al., 2015. The ocean colour climate change initiative: III A round-robin comparison on in-water bio-optical algorithms. Remote Sens. Environ. 162, 271–294.
Brown, T., Simpson, J., 2001. Managing phosphorus inputs to urban lakes. Urban Lake Manage. 3, 771–781.
Carlson, R.E., 1977. A trophic state index for lakes. Limnol. Oceanogr. 22 (2), 361–369.
Carvalho, L., McDonald, C., de Hoyos, C., Mischke, U., Phillips, G., Borics, G., Poikane, S., Skjelbred, B., Solheim, A.L., van Wichelen, J., Cardoso, A.C., Cadotte, M., 2013. Sustaining recreational quality of European lakes: minimizing the health risks from algal blooms through phosphorus control. J. Appl. Ecol. 50, 315–323. https://doi.org/10.1111/1365-2664.12059.
Cavalli, R., Laneve, M.G., Fusilli, L., Pignatti, S., Santini, F., 2009. Remote sensing water observation for supporting Lake Victoria weed management. J. Environ. Manage. 90, 2199–2211.
Chapman, J.L., Chapman, C.A., Kaufman, L., Witte, F., Balirwa, J., 2008. Biodiversity conservation in African inland waters: lessons of the Lake Victoria region. Vereinigung Limnology 30, 16–34.
Chavula, G., Brezonik, P., Thenkabail, P., Johnson, T., Bauer, M., 2009. Estimating chlorophyll concentration in Lake Malawi from MODIS satellite imagery. Phys. Chem. Earth 34, 755–760. https://doi.org/10.1016/j.pce.2009.07.01.
Chen, J., Quan, W., 2013. An improved algorithm for retrieving chlorophyll-a from the Yellow River Estuary using MODIS imagery. Environ. Monit. Assess. 185, 2243–2255. https://doi.org/10.1007/s10661-012-2705-y.
Clarke, G.L., Ewing, G.C., Lorenzon, C.J., 1970. Spectra of backscatterd light from the sea obtained from aircraft as a measure of chlorophyll concentration. Science 167, 119–121.
Coble, P.G., Hu, C., Gould, R., Chang, G., Wood, A.M., 2004. Colored dissolved organic matter in the coastal ocean–An optical tool for coastal zone environmental assessment and management. Oceanography. 17, 50–59.
Dahanayaka, D. D. G. L., Tonooka, H., Wijeyaratne, M. J. S., Minato, A., Ozawa, S., 2014. Assessing the potential of satellite and ground spectral data for Chlorophyll-a monitoring in Lake Kasumigaura, Japan. In Proceedings of the International Geoscience and Remote Sensing Symposium (IGARSS), (December 2013), 3350–3353. http://dx.doi.org/10.1109/IGARSS.2014.6947198.
Dekker, A.G., Malthus, T.J., Seyhan, E., 1991. Quantitative modeling of inland water-quality for high-resolution MSS systems. IEEE Trans. Geosci. Remote Sens. 29, 89–95.
Dörnhöfer, K., Oppelt, N., 2016. Remote sensing for lake research and monitoring – Recent advances. Ecol. Indic. 64, 105–122. https://doi.org/10.1016/j.ecolind.2015.12.009.
Duan, H., Zhang, Y., Zhang, B., Song, K., Wang, Z., Liu, D., Li, F., 2008. Estimation of chlorophyll-a concentration and trophic states for inland lakes in Northeast China from Landsat TM data and field spectral measurements. Int. J. Remote Sens. 29 (3), 767–786. https://doi.org/10.1080/01431160701355249.
Duan, H., Ronghua, M., Chuanmin, H., 2012. Evaluation of remote sensing algorithms for cyanobacterial pigment retrievals during spring bloom formation in several lakes of East China. Remote Sens. Environ. 126, 126–135. https://doi.org/10.1016/j.rse.2012.08.011.
Erkkilä, A., Kalliola, R., 2007. Spatial and temporal representativeness of water monitoring efforts in the Baltic Sea coast of SW Finland. Fennia 185, 107–132.
Esaias, W.E., Abbott, M.R., Barton, I., Brown, O.B., Campbell, J.W., Carder, K.L., Clark, D.K., Evans, R.H., Hoge, F.E., Gordon, H.R., Balch, W.M., Letelier, R., Minnett, P.J., 1998. An overview of MODIS capabilities for ocean science observations. IEEE Trans. Geosci. Remote Sens. 36, 1250–1265.
Fuli, Y. et al. Correlation analysis of spectral reflectance in determining preliminary algorithms for water quality monitoring in Taihu Lake, China, IGARSS 2004. 2004 IEEE International Geoscience and Remote Sensing Symposium, Anchorage, AK, 2004, pp. 4889-4892 vol.7. http://dx.doi.org/10.1109/IGARSS.2004.1370259
Galvez-Cloutier, R., Sanchez, M., 2007. Trophic status evaluation for 154 lakes in Quebec, Canada: monitoring and recommendations. Water Qual. Res. J. Can. 42 (4), 252–268.

Garaba, S., Voß, D., Zielinski, O., 2014. Physical, bio-optical state and correlations in north-western european shelf seas. Remote Sens. 6, 5042–5066. https://doi.org/10.3390/rs6065042.

Garaba, S., Zielinski, O., 2015. An assessment of water quality monitoring tools in an estuarine system. Remote Sens. Appl. Soc. Environ. 2, 1–10.

Giardino, C., Oggioni, A., Bresciani, M., Yan, H., 2010. Remote sensing of suspended particulate matter in Himalayan lakes. Mt Res. Dev. 30, 157–168. https://doi.org/10.1659/MRD-JOURNAL-D-09-00042.1.

Gidudu, A., Mugo, R., Letaru, L., Wanjohi, J., Nakibule, R., Adams, E., Flores, A., Page, B., Okello, W., 2018. Evaluation of satellite retrievals of water quality parameters for Lake Victoria in East Africa. Afr. J. Aquat. Sci. 43 (2), 141–151. https://doi.org/10.2989/16085914.2018.1446899.

Gitelson, A.A., Yacobi, Y.Z., Karnieli, A., Kress, N., 1996. Reflectance spectra of polluted marine waters in Haifa Bay, Southeastern Mediterranean: features and application for remote estimation of chlorophyll concentration. Isr. J. Earth Sci. 45, 127–136.

Gómez-Jakobsen, F., Mercado, M.J., Cortés, D., Ramírez, T., Salles, S., Yebra, L., 2016. A new regional algorithm for estimating chlorophyll-a in the Alboran Sea (Mediterranean Sea) from MODIS-Aqua satellite imagery. Int. J. Remote Sens. 37 (6), 1431–1444. https://doi.org/10.1080/01431161.2016.1154223.

Gordon, H.R., Morel, A.Y., 1983. Remote assessment of ocean color for interpretation of satellite visible imagery—A review. In: Barber, R.-.-T., Mooers, C.-.-N.-.-K., Bowman, M.J., Zeitzschel, B. (Eds.), Lecture notes on Coastal and Estuarine Studies 4. Springer Verlag, New York.

Gordon, H.R., Wang, M., 1994. Retrieval of water-leaving radiance and aerosol optical thickness over the oceans with SeaWiFS: a preliminary algorithm. Appl. Opt. 33, 443–452.

Gordon, H.R., Clark, D.K., Brown, J.W., Brown, O.B., Evans, R.H., Broenkow, W.W., 1983. Phytoplankton pigment concentrations in the Middle Atlantic Bight: comparison of ship determinations and CZCS estimates. Appl. Opt. 22, 20–36.

Gurlin, D., Gitelson, A.A., Moses, J.W., 2011. Remote estimation of chl-a concentration in turbid productive waters — Return to a simple two-band NIR-red model?. Remote Sens. Environ. 115, 3479–3490. https://doi.org/10.1016/j.rse.2011.08.011.

Han, L., Jordan, K., 2005. Estimating and mapping chlorophyll-a concentration in Pensacola Bay, Florida using Landsat ETM+ data. Int. J. Remote Sens. 26 (23), 5245–5254.

Harma, P., Vepsäläinen, J., Hannonen, T., Pyhälahti, T., Kamari, J., Kallio, K., Eloheimo, K., Koponen, S., 2001. Detection of water quality using simulated satellite data and semi empirical algorithms in Finland. Sci. Total Environ. 268, 107–121.

Hestir, E.L., Brando, V.E., Bresciani, M., Giardino, C., Matta, E., Villa, P., Dekker, A.G., 2015. Measuring freshwater aquatic ecosystems: the need for a hyperspectral global mapping satellite mission. Remote Sens. Environ. 167, 181–195. https://doi.org/10.1016/j.rse.2015.05.023.

Hooker, S.B., McClain, C.R., 2000. The calibration and validation of SeaWiFS data. Prog. Oceanogr. 45, 427–465.

Hu, C., Lee, Z., Franz, B.A., 2012. Chlorophyll-a algorithms for oligotrophic oceans: a novel approach based on three-band reflectance difference. J. Geophys. 117, C01011. https://doi.org/10.1029/2011JC007395.

ISO10260:1992. Water quality–Measurement of Biochemical Parameters–Spectrometric Determination of the Chlorophyll a Concentration. Technical Committee: ISO/TC 147/SC 2 Physical, Chemical and Biochemical Methods.

Jiao, H.B., Zha, Y., Gao, J., Li, Y.M., Wei, Y.C., Huang, J.Z., 2006. Estimation of chlorophyll – A concentration in Lake Tai, China using situ hyperspectral data. Int. J. Remote Sens. 27 (19), 4267–4276.

Kahru, M., Kudela, R., Anderson, C., Manzano-Sarabia, M., Mitchell, B., 2014. Evaluation of satellite retrievals of ocean chlorophyll a in the California current. Remote Sens. 6, 8524–8540.

Lacava, T., Ciancia, E., Di Polito, C., Madonia, A., Pascucci, S., Pergola, N., Piermattei, V., Satriano, V., Tramutoli, V., 2018. Evaluation of MODIS—Aqua chlorophyll-a algorithms in the basilicata ionian coastal waters. Remote Sens. 10, 987. https://doi.org/10.3390/rs10070987.

Laliberté, J., Larouche, P., Devred, E., Craig, S., 2018. Chlorophyll-a concentration retrieval in the optically complex waters of the St. Lawrence estuary and gulf using principal component analysis. Remote Sens. 10, 265. https://doi.org/10.3390/rs10020265.

Lesht, B.M., Barbiero, R.P., Warren, J.G., 2012. Satellite ocean color algorithms: a review of applications to the Great Lakes. J. Great Lakes Res. 38, 49–60. https://doi.org/10.1016/j.jglr.2011.10.005.

Lesht, B.M., Barbiero, R.P., Warren, J.G., 2013. A band-ratio algorithm for retrieving open-lake chlorophyll values from satellite observations of the Great Lakes. J. Great Lakes Res. 39, 138–152. https://doi.org/10.1016/j.jglr.2012.12.007.

Lessin, G., Ossipova, V., Lips, I., Raudsepp, U., 2009. Identification of the coastal zone of the central and eastern Gulf of Finland by numerical modeling, measurements, and remote sensing of chlorophyll a. Hydrobiologia 629, 187–198. https://doi.org/10.1007/s10750-009-9770-4.

Li, S., Wu, Q., Wang, X., Piao, X., Dai, Y., 2002. Correlation between reflectance spectra and contents of chlorophyll-a in Chaohu Lake. J. Lake Sci. 14, 228–234.

Lillesand, T.M., Kiefer, R., 1994. Remote Sensing and Image Interpretation. 3rd edition. USA.

Matthews, W.M., 2011. A current review of empirical procedures of remote sensing in inland and near-coastal transitional waters. Int. J. Remote Sens. https://doi.org/10.1080/01431161.2010.512947.

Matthews, M.W., Bernard, S., Winter, K., 2010. Remote sensing of cyanobacteria-dominant algal blooms and water quality parameters in Zeekoevlei, a small hypertrophic lake, using MERIS. Remote Sens. Environ. 114 (9), 2070–2087. https://doi.org/10.1016/j.rse.2010.04.013.

Matthews, M., Bernard, S., Robertson, L., 2012. An algorithm for detecting trophic status (chlorophyll-a), cyanobacterial dominance, surface scums and floating vegetation in inland and coastal waters. Remote Sens. Environ. 124, 637–652.

McClain, C.R., 2009. A decade of satellite ocean color observations. Annu. Rev. Mar. Sci. 1, 19–42.

Morel, A., Prieur, L., 1977. Analysis of variations in ocean color. Limnol. Oceanogr. 22, 709–722.

Morel, A., 2001. Bio-optical Models. Encyclopedia of Ocean Sciences. Oxford: Academic Press. http://dx.doi.org/10.1006/rwos.2001.0407.

Moses, J.W., Gitelson, A.A., Berdnikov, S., Povazhnyy, V., 2009. Estimation of chlorophyll-a concentration in case II waters using MODIS and MERIS data—successes and challenges. Environ. Res. Lett. 4,. https://doi.org/10.1088/1748-9326/4/4/045005 045005.

Mueller, J.L., 2000. SeaWiFS algorithm for the diffuse attenuationcoefficient, K (490), using water-leaving radiances at 490 and 555 nm. In: SeaWiFS Postlaunch Calibration and Validation Analyses, Part 3, NASAGoddard Space Flight Cent, Greenbelt, USA, 11: 24-27.

Murthy, P.G., Shivalingaiah, Leelaja, Hosmani P.S., 2008. Trophic State Index in Conservation of Lake Ecosystems. In Proceedings of the 12th World Lake Conference. Jaipur, Rajasthan, India. 840-843.

Mustapha, S.D., Bélanger, S., Larouche, P., 2012. Evaluation of ocean color algorithms in thesouth-eastern Beaufort Sea, Canadian Arctic: New parameterization using SeaWiFS, MODIS, and MERIS spectral bands. Can. J Remote Sens. 38, 535–556.

Nasr, H.A., Belal, M.L., Ashraf, K.H., 2007. Assessment of Some Water Quality Parameters Using MODIS Data along the Red Sea Coast, Egypt. ICGST-GVIP Journal 7, 26–30.

Naumann, E., 1929. The Scope of chief problems of regional limnology. Internationale Revue der gesamten Hydrobiologie und Hydrographie. 22, 423–444.

Navalgund, R.R., Jayaraman, V., Roy, P.S., 2007. Remote sensing applications: an overview. Curr. Sci. 93, 1747–1766.

Nürnberg, G., 1996. Trophic state in clear and colored, soft- and hardwater lakes with special consideration of nutrients, anoxia, phytoplankton and fish. Lake Reserv. Manage. 12 (4), 432–447.

O'Reilly, J.E, Maritorena, S., O'Brien, M.C., Siegel, D.A., Toole, D., Menzies, D., Smith, R. C., Mueller, J.L., Mitchell, B.G., Kahru, M., et al. 2000. SeaWiFS Postlaunch Calibration and Validation Analyses, Part 3; NASA Technical Memorandum 2000–206892; NASA Goddard Space Flight Center: Greenbelt, MD, USA, May; pp1–49.

O'Reilly, J.E., Maritorena, S., Mitchell, B.G., Siegel, D.A., Carder, K.L., Garver, S.A., Kahru, M., McClain, C.R., 1998. Ocean color chlorophyll algorithms for SeaWiFS. J. Geophys. 103, 24937–24953.

OECD (Organization for Economic Cooperation and Development). 1982. Eutrophication of waters. Monitoring, assessment and control. Final report, OECD cooperative programme on monitoring of inland waters (eutrophication control), Environment Directorate, OECD, Paris. 154.

Olmanson, L.G., Brezonik, P.L., Bauer, E.M., 2011. Evaluation of medium to low resolution satellite imagery for regional lake water quality assessments. Water Resour. Res. 47, W09515. https://doi.org/10.1029/2011WR011005.

Prasad, A.G., Siddaraju, 2012. Carlson's Trophic State Index for the assessment of trophic status of two Lakes in Mandya district. Adv Appl Sci Res., 2012. 3 (5), 2992-2996 ISSN: 0976-8610.

Reyjol, Y., Argillier, C., Bonne, W., Borja, A., Buijse, A.D., Cardoso, A.C., Daufresne, M., Kernan, M., Ferreira, M.T., Poikane, S., Prat, N., Solheim, A.L., Stroffek, S., Usseglio-Polatera, P., Villeneuve, B., van de Bund, W., 2014. Assessing the ecological status in the context of the European Water Framework Directive: where do we go now?. Sci. Total Environ. 497–498, 332–344. https://doi.org/10.1016/j.scitotenv.2014.07.119.

Ritchie, J.C., Zimba, P.V., Everitt, J.H., 2003. Remote sensing techniques to assess water quality. Photogramm. Eng. Remote Sci. 69 (6), 695–704.

Rocchini, R. and Swain, L. G. 1995. The British Columbia Water Quality Index, Water Quality Branch, EP Department, B.C., Ministry of Environment, Land and Park, Victoria, B.C., Canada.13 pp.

Rundquist, D.C., Han, L., Schalles, J.F., Peake, J.S., 1996. Remote measurement of algal chlorophyll in surface waters: the case for the first derivative of reflectance Near 690 nm. Photogramm Eng Rem S. 62 (2), 195–200.

Schaeffer, A., Schaeffer, B.K., Darryl, K., Lunetta, R.S., Conmy, R., Gould, R.W., 2013. Barriers to adopting satellite remote sensing for water quality management. Int. J. Remote Sens. 34 (21), 7534–7544.

Schalles, J.F., Gitelson, A., Yacobi, Y.Z., Kroenke, A.E., 1998. Estimation of chlorophyll A from time series measurements of high spectral resolution reflectance in an eutrophic lake. J. Phycol. 34 (2), 383–390. https://doi.org/10.1046/j.1529-8817.1998.340383.x.

Stainton M.P., Capel M. J., and Armstrong F. A. J. 1977. The chemical analysis of fresh water. Canada Fisheries and Marine Service. Miscellaneous special publications.

Thiemann, S., Kaufmann, H., 2000. Determination of chlorophyll content and trophic state of lakes using field spectrometer and IRS-1C satellite data in the Mecklenburg Lake District, Germany. Remote Sens. Environ. 73 (2), 227–235.

Tian, G.L., Ni, X.D., 1988. Estimating chlorophyll concentration using spectral data. Remote Sens. Environ. 3, 71–79.

Wang, M., Nim, J.C., SeungHyun, S., Wei, S., 2012. Characterization of turbidity in Florida's lake okeechobee and caloosahatchee and St. lucie estuaries using MODIS-aqua measurements. Water Res. 46, 5410–5422.

Watanabe, F., Alcântara, E., Imai, N., Rodrigues, T., Bernardo, N., 2018. Estimation of chlorophyll-a concentration from optimizing a semi-analytical algorithm in productive inland waters. Remote Sens. 10, 227. https://doi.org/10.3390/rs10020227.

Werdell, P.J., Bailey, S.W., 2005. An improved in situ bio-optical data set for ocean color algorithm development and satellite data product validation. Remote Sens. Environ. 98, 122–140.

Zheng, G.D., Giacomo, P.M., 2017. Uncertainties and applications of satellite-derived coastal water quality products. Prog. Oceanogr. 2017 (159), 45–72.

Zhengjun, W., Jianming, H., Guisen, D., 2008. Use of satellite imagery to assess the trophic state of Miyun Reservoir, Beijing, China. Environ Pollut. 155, 13–19. https://doi.org/10.1016/j.envpol.2007.11.003.

Ziboon, A.R.T., Al Zubaidy, R.Z., Al Khafaj, S.M., 2010. Remote sensing model for monitoring trophic state of al huweizah marsh. Eng. Tech. J. 28.